18-mN XENON ION PROPULSION SUBSYSTEM*

J.R. Beattie,** R.R. Robson,† and J.D. Williams††

Hughes Research Laboratories

Malibu, California 90265

USA

ABSTRACT

This paper describes an 18-mN xenon ion propulsion subsystem (XIPS) under development for north-south stationkeeping (NSSK) of three-axis- and spin-stabilized communications satellites. The XIPS consists of a 13-cm-diam thruster, a power supply, and a xenon storage and control unit. The thruster produces 17.8 mN of thrust at a specific impulse of 2585 s, with an input power of about 439 W. This high level of performance is achieved using a ring-cusp magnetic field arrangement to confine the discharge-chamber plasma, and a three-grid ion optics assembly to extract the thrust beam. The power supply contains only 400 parts in its 7 individual modules: screen, accel, discharge, 2 keepers, and 2 heaters. The power supply is designed to operate from a 29- to 34-V power bus, and achieves an overall efficiency of 88 to 90% over this range. Xenon propellant is stored at an initial pressure of 7.6 MPa (1100 psia) to give a tankage fraction of only about 12%. Control of the xenon flow rates is accomplished using a pressure regulator to reduce the storage pressure to 68.9 kPa (10 psia) on the upstream side of flow restrictors located in the lines leading to the discharge and neutralizer cathodes and the discharge chamber. We present the performance and operating characteristics of laboratory- and engineering-model XIPS thrusters operated with a breadboard-model power supply and a laboratory-model flow control system.

NOMENCLATURE

d_a = accel aperture diameter, mm
D_B = active beam diameter, cm
d_d = decel aperture diameter, mm
d_s = screen aperture diameter, mm
F = thrust, mN
I_{sp} = specific impulse, s
J_A = accel electrode current, mA
J_b = beam current, A
J_{ck} = cathode keeper current, A
J_d = decel electrode current, mA
J_E = cathode emission current, A
J_{nk} = neutralizer keeper current, A
l_e = effective acceleration length, mm
l_g = electrode spacing, mm
m_c = cathode flow rate, mA
m_m = main flow rate, A
m_n = neutralizer flow rate, mA
P_T = thruster input power, W
P_{tk} = vacuum chamber pressure, Pa
R_{max} = maximum ratio of beam-to-total voltage
V_A = accelerator voltage, V
V_b = beam voltage, V
V_{ck} = cathode keeper voltage, V
V_D = discharge voltage, V
V_g = neutralizer coupling voltage, V
V_{nk} = neutralizer keeper voltage, V
t_a = accel electrode thickness, mm
t_d = decel electrode thickness, mm
t_s = screen electrode thickness, mm
γ = thrust loss factor
ε_i = beam ion production cost, W/A
η_e = thruster electrical efficiency, %
η_m = total propellant utilization efficiency, %
η_{md} = dischg. propellant utilization efficiency, %
η_T = thruster efficiency, %

INTRODUCTION

Previous publications[1-3] have described the performance advantages and development status of the 63.5-mN XIPS that we developed for NSSK applications on large spin-stabilized communications satellites.

*Work performed under company funding.
**Project Manager, Plasma Physics Department. Senior Member AIAA.
†Head, Power Electronics and Controls Section, Plasma Physics Department. Member AIAA.
††Member of the Technical Staff, Plasma Physics Department. Member AIAA.

At its nominal operating point, the 25-cm-diam XIPS thruster operates with an input power of P_T = 1.3 kW to achieve a specific impulse of I_{sp} = 2800 s and a thruster efficiency of η_T = 65%. We have also documented the performance of this thruster under high-power operating conditions,[3] in which it operates with an input power of P_T = 4.5 kW to produce 179 mN of thrust at a specific impulse of I_{sp} = 4000 s and a thruster efficiency of η_T = 78%.

Our analysis of the optimum thruster size for use on smaller spin-stabilized and three-axis-stabilized satellites has indicated that a 13-cm-diam unit producing about 18 mN of thrust is optimal. In scaling to the smaller size, we held the thrust density (beam current density) constant, so that the wearout rates anticipated in the smaller thruster would be approximately the same as those that were encountered in the wear mechanism test of our 25-cm-diam thruster. In that test,[3] in which we successfully completed 4350 h of cyclic operation, the primary wearout mechanism in the XIPS thruster was identified as enlargement of the accelerator apertures due to charge exchange ion erosion. Implicit in our expectation that the wearout rate in the smaller thruster will be approximately the same as that of the larger thruster is the assumption that the scaled unit can operate at about the same discharge voltage and propellant utilization efficiency as the larger one.

In the remainder of this paper, we describe the 18-mN XIPS that we are developing, which consists of a 13-cm-diam thruster, a simplified power supply, and a xenon storage and control system. We also discuss the performance characteristics of both laboratory- and engineering-model XIPS thrusters and a breadboard-model power supply, and we describe our plans to flight-qualify the XIPS thruster.

XENON ION PROPULSION SUBSYSTEM

Figure 1 is a schematic diagram of the XIPS. This compact arrangement of a 13-cm-diam thruster, its power supply, and its propellant tankage and control unit is one-half of a fully redundant propulsion system intended for use on small spin-stabilized satellites. For three-axis-stabilized satellites, a typical arrangement would consist of four thrusters and power supplies, and two propellant tanks. A mass breakdown for this latter configuration is provided in Table 1.

With an input power of 439 W, the XIPS thruster produces 17.8 mN of thrust at a specific impulse of 2585 s, resulting in a thrust-to-power ratio of 40.6 mN/kW and a thruster efficiency of over 51%. We believe this to be the highest level of performance ever reported for an ion thruster of this size operated at a discharge voltage of only 28 to 30V.

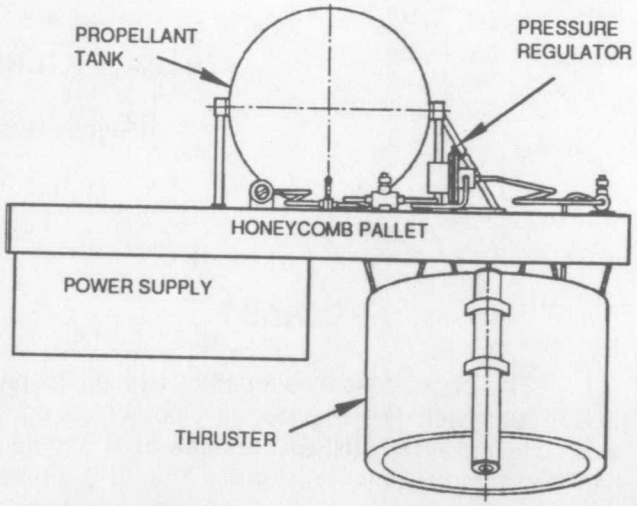

Fig. 1. Xenon ion propulsion subsystem (XIPS).

The xenon propellant is stored as a high-pressure gas, with a density about twice that of water. The flow of xenon into the thruster is passively controlled, using a pressure regulator to maintain a constant pressure on the upstream side of flow restrictors located in the propellant lines leading to the discharge chamber, its cathode, and the neutralizer cathode.

The power supply requires an input power of about 500 W and can operate over a spacecraft bus voltage range of either 28.9 V to 34 V or 49 V to 53 V. The unit is completely self-contained and includes all the timing and control required to start, stop, and operate the thruster, as well as to detect and implement corrective actions in the event of overcurrent conditions in the screen or accelerator power modules. The maximum output voltage of the power supply is provided by the screen module, which requires an output of only 750 V to give xenon ions an exhaust velocity equivalent to about 3390-s specific impulse (uncorrected for propel-

Table 1. XIPS Mass Estimates.

UNIT	UNIT MASS (kg)	NO. PER SPACECRAFT	MASS PER SPACECRAFT
ION THRUSTER	5.0	4	20.0
POWER PROCESSOR UNIT	6.8	4	27.2
XENON TANK	2.0	2	4.0
PRESSURE REGULATOR	0.8	2	1.6
OTHER FEED COMPONENTS	3.5	–	3.5
GIMBAL	2.2	4	8.8
STRUCTURE	2.8	–	2.8
TOTAL MASS			67.9

lant utilization efficiency and thrust loss due to beam divergence and doubly charged ions). The low output voltage of the XIPS power supply simplifies spacecraft integration and voltage isolation.

We are in the process of completing two working-model systems containing the essential features of the XIPS shown in Fig. 1. They consist of qualification-model thrusters, breadboard-model power supplies, and a flight-prototype pressure regulator. Detailed discussions of the individual elements of the XIPS are presented in the sections that follow.

THRUSTER

Figure 2 is a cutaway drawing of the 13-cm-diam XIPS thruster. The thruster is scaled from the 25-cm-diam XIPS design, which was derived from the original ring-cusp configuration developed by Sovey.[4] The discharge chamber employs a central hollow cathode equipped with an enclosed-type keeper electrode. Xenon enters the discharge chamber through an annular plenum, which distributes the propellant uniformly throughout the ionization volume. A magnetic field used to confine the discharge electrons is produced by three rings of $SmCo_5$ permanent magnets located on the cylindrical sidewall and circular endwall. The resulting scalar magnetic field geometry is presented in Fig.3, which illustrates the strong fields that exist at the anode-potential boundaries formed by the sidewall and endwall. By comparison, a relatively weak field exists throughout most of the discharge volume and at the cathode-potential boundary formed by the screen electrode.

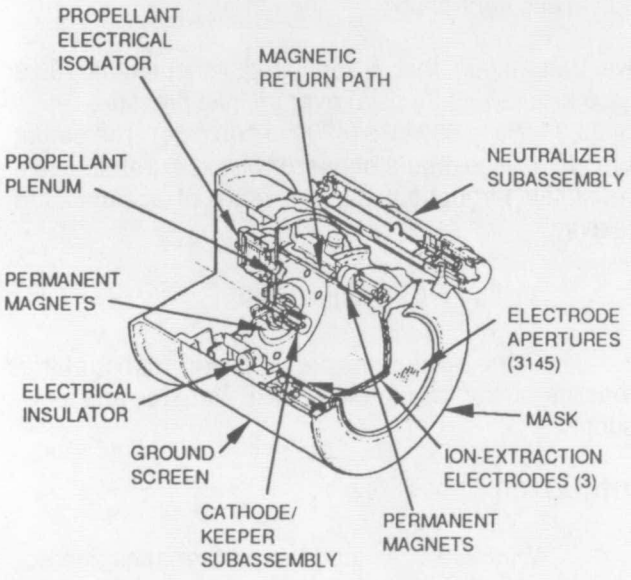

Fig. 2. 13-cm-diam thruster.

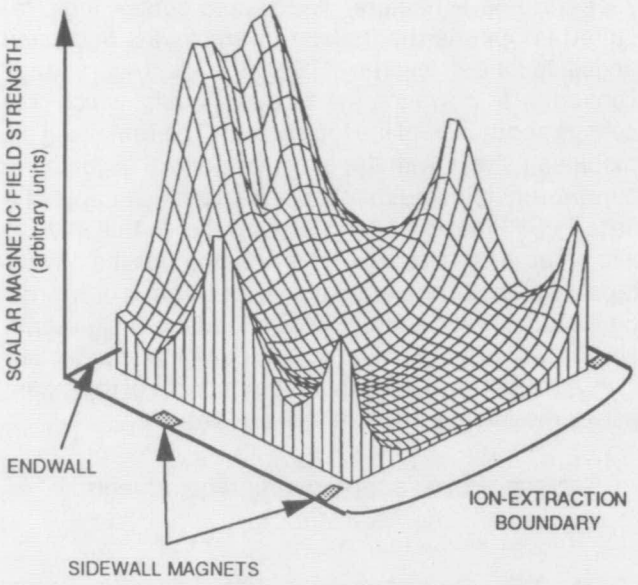

Fig. 3. Magnetic field geometry.

A three-grid ion extraction assembly is used to extract, focus, and vector the 3125 individual beamlets that form the thrust beam. With the exception of the cathode, keeper, and screen electrode, the entire interior of the discharge chamber is maintained at anode potential. Electrons for neutralizing the positive ion beam are provided by the neutralizer assembly, which was also scaled from the 25-cm-diam XIPS thruster.

POWER SUPPLY

Figure 4 is a block diagram of the breadboard-model power supply. The power supply contains the

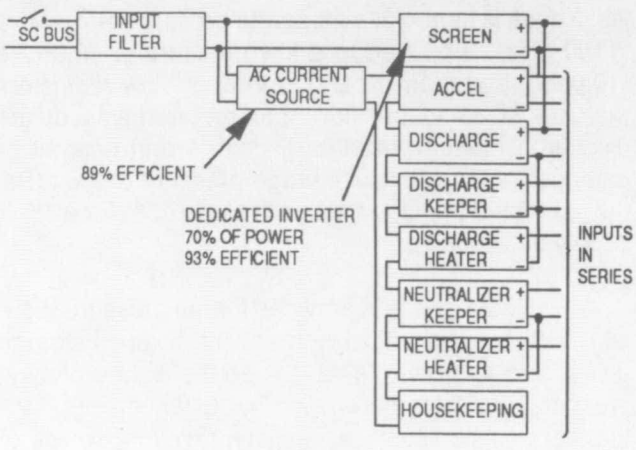

Fig. 4. Block diagram of power supply.

seven power modules (screen, accel, discharge, 2 keepers, and 2 heaters) and simple control logic required to operate the thruster. It employs a dedicated series resonant inverter (SRI) as a dc-to-dc voltage converter for powering the screen module, which processes about 70% of the total power. The remaining six modules (which, with the exception of the accel, have current-regulated outputs) operate from the output of a second SRI that is used to convert the dc bus voltage into an ac current source. This scheme has the advantage that the current regulation is performed only once (in the ac current source), which leads to a significant simplification in the power supply design and reduction in its parts count. The output requirements of the seven power modules are summarized in Table 2.

Table 2. Power supply output requirements.

POWER SUPPLY MODULE	MAXIMUM OUTPUT		NOMINAL OUTPUT			REGULATION	
	V	A	V	A	W	E or I	%
SCREEN	750	0.5	750	0.4	303	E	≤5
ACCELERATOR	300	0.01	300	0.001	0.3	E	≤5
DISCHARGE	50	4.0	30	3.4	102	I	≤5
DISCHARGE KEEPER	30	1.0	19	1.0	19	I	≤5
DISCHARGE HEATER	20	3.5	–	–	–	I	≤5
NEUTRALIZER KEEPER	30	1.0	19	1.0	19	I	≤5
NEUTRALIZER HEATER	20	3.5	–	–	–	I	≤5
TOTAL POWER	–	–	–	–	443	–	–

XENON STORAGE AND CONTROL UNIT

Figure 5 is a block diagram of the propellant tankage and control unit configured for a typical four-thruster arrangement on a three-axis-stabilized satellite. Xenon is stored at a moderate pressure of 7.6 MPa (1100 psia), regulated to a low pressure of 68.9 kPa (10 psia), and then expanded through flow restrictors that are sized to the flow rate requirements of the discharge plenum and the discharge and neutralizer cathodes. With an initial storage pressure of 7.6 MPa, the estimated tankage fraction is about 15% for a 15-yr supply of Xenon.

Redundancy is provided for the pressure regulator, which is the critical element of the xenon storage and control system. We have used the flight-prototype pressure regulator shown in Fig. 6 for testing XIPS thrusters since 1985, accumulating well in excess of 5000 h of operating time. In initial testing of the regulator,

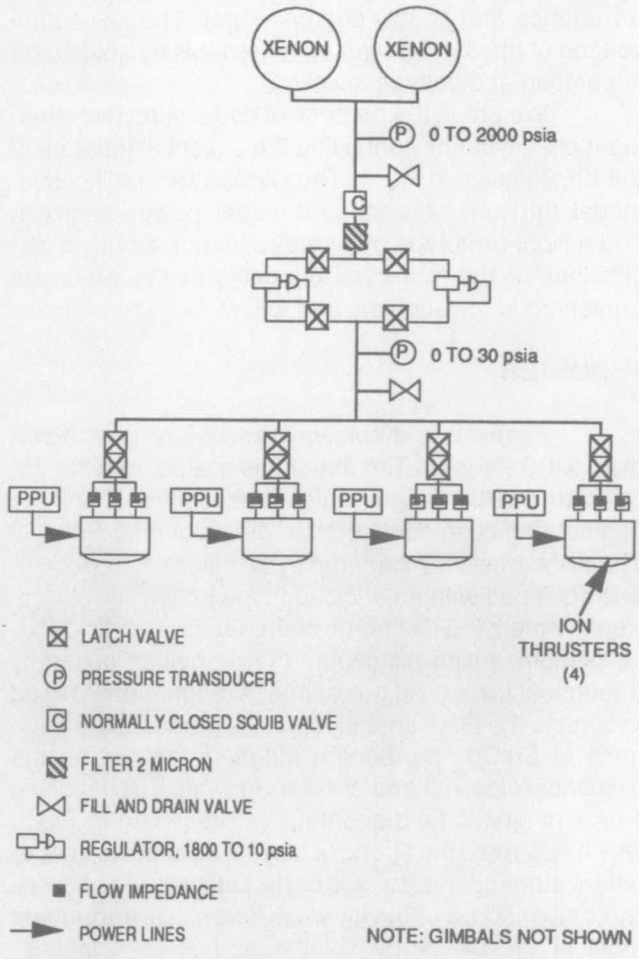

Fig. 5. Block diagram of propellant storage and control unit.

we determined that it regulated its output to 68.9 ±2.5 kPa (10 ±0.36 psia) over an inlet pressure range of 28.9 MPa to 689 kPa (4200 to 100 psia). The output pressure of the regulator has remained extremely well-regulated throughout the six years of accumulated testing.

PERFORMANCE

In this section, we present performance characteristics of the 13-cm-diam XIPS thruster and power supply.

THRUSTER

We have evaluated the performance characteristics of both laboratory and engineering models of the 13-cm-diam XIPS thruster. Figure 7 is a schematic of a laboratory-model thruster which simulates the

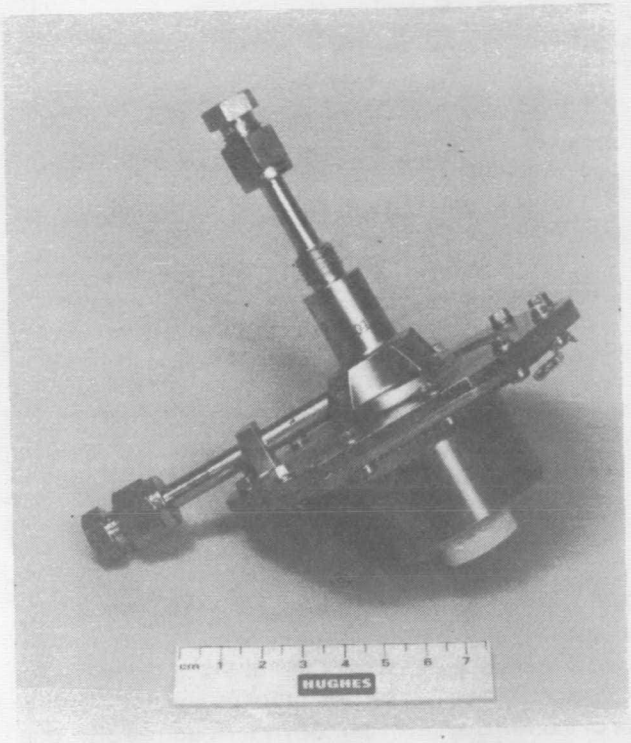

Fig. 6. Flight-prototype pressure regulator.

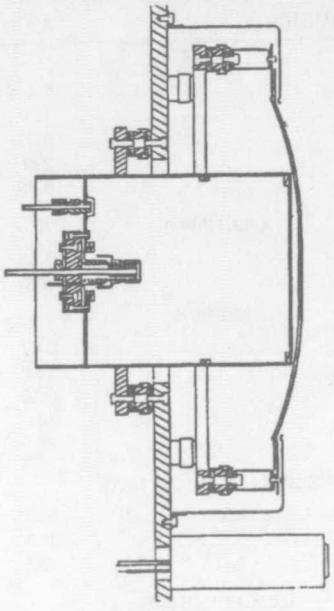

Fig. 7. Laboratory-model thruster.

overall arrangement and critical dimensions of the flight-model XIPS design. However, as an expediency, the laboratory-model thruster employs an oversized (30-cm-diam) ion extraction assembly (designated as S/N 917)that has the electrode and aperture geometries listed in Table 3. Performance data obtained with the lab-model thruster are presented in Fig. 8, confirming the high level of performance anticipated for the ring-cusp discharge chamber and the performance improvement resulting from operation at higher discharge voltage.

Table 3. Ion Optics Dimensions.

OPTICS S/N	D_B (cm)	d_s (mm)	d_a (mm)	d_d (mm)	t_s (mm)	t_a (mm)	t_d (mm)
917	28.5	1.91	1.14	*	0.25	0.38	*
100	6.2	1.91	1.14	1.52	0.25	0.25	0.25
101	6.2	1.91	1.14	1.52	0.25	0.51	0.25

* TWO-GRID SYSTEM

We have also documented the discharge chamber performance of an engineering-model thruster, which employs a discharge chamber that is essentially identical to the flight-model XIPS design, and which was fabricated and assembled as flight hardware (the discharge chamber is one of two simulators that are described later in this paper). The engineering-model thruster was tested using ion extraction assemblies that we have fabricated for use on the qualification-model XIPS thrusters that are described in a later section. The electrode and aperture geometries of these ion optics (designated as S/N 100 and S/N 101) are listed in Table 3 . For expediency, we utilized a

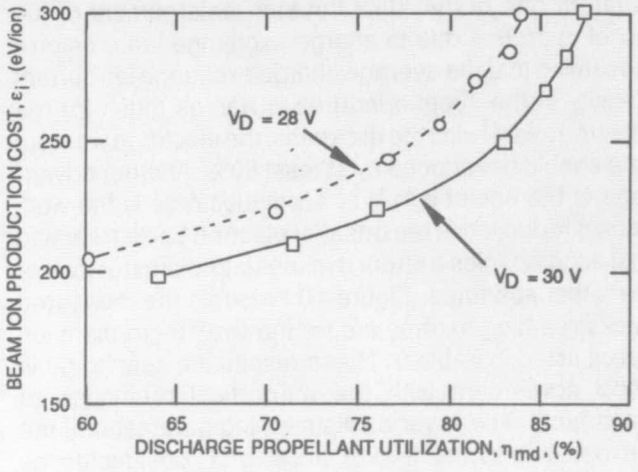

Fig. 8. Performance of lab-model thruster.

laboratory-model neutralizer for conducting the discharge chamber and ion optics performance evaluations discussed in the sections that follow.

Performance data obtained with the engineering-model thruster are presented in Fig. 9. Comparison of these results with those of Fig. 8 indicates a significant increase in the performance of the engineering-model thruster over that of the laboratory-model unit. We attribute this performance enhancement to the use of the smaller ion optics assemblies, which eliminate the loss of un-ionized propellant that is believed to occur beyond the 13.2-cm-diam active beam boundary

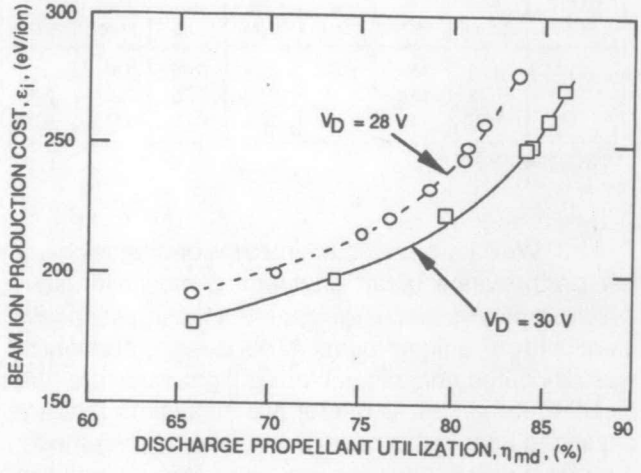

Fig. 9. Performance of engineering-model thruster.

in the larger ion extraction assembly.

The ion optics designated as S/N 101 in Table 3 employ a thicker accel electrode to reduce the known wearout rate of the XIPS thruster: enlargement of the accel apertures due to charge exchange ion erosion.[3] Assuming that the average charge exchange ion current density in the accel apertures is half as much for the electrode with twice the thickness, the electrode wearout rate should be reduced by at least 50%. Another advantage of the use of a thicker accel electrode is the well-known reduction in the onset of electron backstreaming that accompanies a larger thickness-to-diameter ratio of the accel apertures. Figure 10 presents the measured backstreaming parameters for the two 13-cm-diam ion optics listed in Table 3. These results are seen to be in good agreement with the theoretical prediction of Kaufman.[5] The lower backstreaming parameter of the ion optics with the thicker accel grid (designated as S/N101) corresponds to a backstreaming limit of only

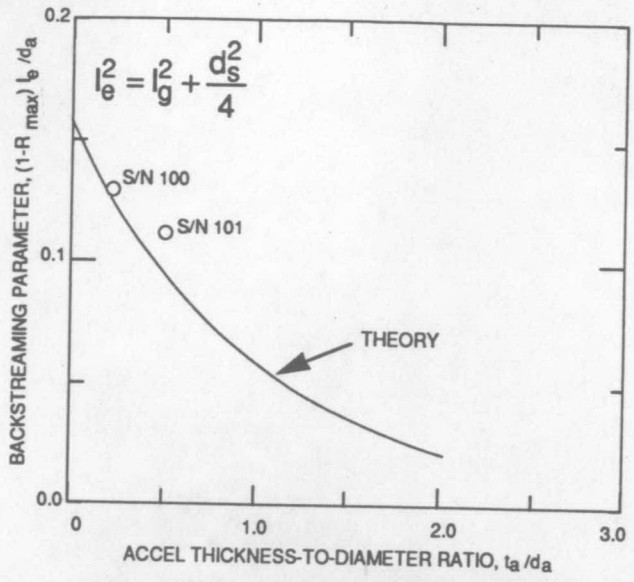

Fig. 10. Backstreaming parameter.

about 125 V, suggesting that the XIPS accelerator voltage could be reduced from its present value of 300 V to as low as ≈200 V. Operation at this reduced accel voltage could be exploited to further reduce the wearout rate of the XIPS accel electrode by as much as 50% due to the corresponding reduction in charge exchange ion sputtering yield.

Table 4 summarizes the thruster electrical parameters and flow rates for the nominal operating point

Table 4. Nominal Operating Conditions of Engineering-Model XIPS Thruster.

OPERATING PARAMETER	VALUE
BEAM	
J_b, A	0.405
V_b, V	751
J_A, mA	0.97
V_A, V	299
J_d, mA	0.49
DISCHARGE	
J_E, A	3.38
V_D, V	30.0
KEEPER	
J_{ck}, A	0.87
V_{ck}, V	18.6
J_{nk}, A	0.50
V_{nk}, V	16
V_g, V	22
PROPELLANT FLOW RATE	
m_m, A	0.446
m_c, mA	35.3
m_n, mA	33.5
TANK PRESSURE	
P_{tk}, Pa	1.3×10^{-4}

of the engineering-model XIPS thruster. In tabulating these data, we made assumptions on the neutralizer performance that can be expected for the 13-cm-diam XIPS thruster, based on the demonstrated characteristics of the 25-cm-diam unit. In Table 5, we summarize the performance of the engineering-model XIPS thruster using the electrical and flow rate conditions of Table 4, and using a value of 0.97 for the thrust-loss factor γ, which accounts for ion beam divergence and doubly charged ions. This is a conservative choice for the parameter γ since it was taken from the 25-cm-diam XIPS thruster and there should be a significantly lower concentration of doubly charged ions in the smaller thruster, which operates at a lower propellant utilization efficiency.

Table 5. Performance of Engineering-Model XIPS Thruster.

OPERATING PARAMETER	VALUE
F, mN	17.8
I_{sp}, s	2585
P_T, W	439
η_m, %	78.7
η_e, %	69.3
η_T, %	51.3

We evaluated the performance sensitivity of the engineering-model thruster to variations in power supply output and xenon flow rates. This was accomplished by establishing thruster operation at the nominal conditions listed in Table 4, and then varying the individual power supply outputs and the cathode and main flow rates by ±10% about the nominal values. A linear least squares curve fit of the resulting data allowed us to calculate performance sensitivities in units of percent change in performance per percent change in the controlled parameters. Sensitivity data determined in this manner are listed in Table 6, showing that the sensitivities in thrust and specific impulse are considerably less than 1% per percent change in operating conditions. This highly desirable stability characteristic of the 13-cm-diam XIPS thruster was also apparent in our larger thruster and considerably reduces the regulation requirements on the XIPS power supply and xenon flow controller.

Table 6. Thruster Performance Sensitivity.

OPERATING PARAMETER	PERFORMANCE SENSITIVITY, % / %	
	THRUST	SPECIFIC IMPULSE
	POWER SUPPLY OUTPUT	
V_b	+0.5	+0.5
V_A	+0.03	0
J_E	+0.7	+0.7
	XENON FLOW RATE	
m_m	+0.7	-0.2
m_c	-0.3	-0.4

POWER SUPPLY

The breadboard-model power supply has been tested using resistive loads to simulate the 13-cm-diam XIPS thruster. Under these conditions, the power supply has an efficiency of approximately 88% for the nominal thruster operating point. This efficiency represents a total power loss of 59.3 W, with the losses distributed as indicated in Table 7. The efficiency of the screen inverter is shown in Fig. 11 for variations in input voltage and output power. It has an efficiency of approximately 93% at its nominal output power of 300 W. The efficiency vs. output power of the ac current source is shown in Fig. 12. It has an efficiency of approximately

Table 7. Power Supply Losses.

NORMAL OPERATION		
SCREEN	22.6	
AC INVERTER	14.0	
ACCEL	2.3	
DISCHARGE	5.7	
CATHODE KEEPER	2.1	
CATHODE HEATER (OFF)	1.2	
NEUTRALIZER KEEPER	2.1	
NEUTRALIZER HEATER (OFF)	1.2	
HOUSEKEEPING	2.7	
INTERNAL WIRING	3.9	
OUTPUT WIRING	0.6	
MISCELLANEOUS	0.9	
TOTAL	59.3	WATTS

EFFICIENCY AT NOMINAL POWER = 88%

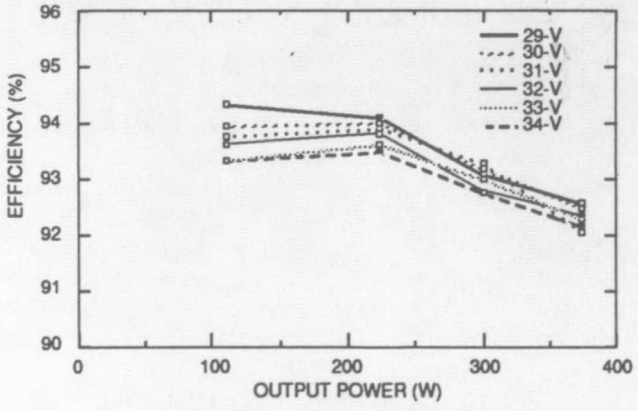

Fig. 11. Efficiency of screen inverter.

89% at its nominal output power of 120 W. The combined line and load regulation of both the screen inverter and the ac current source is better than 1%. We regard this performance as outstanding, especially considering that the power supply contains only 400 parts.

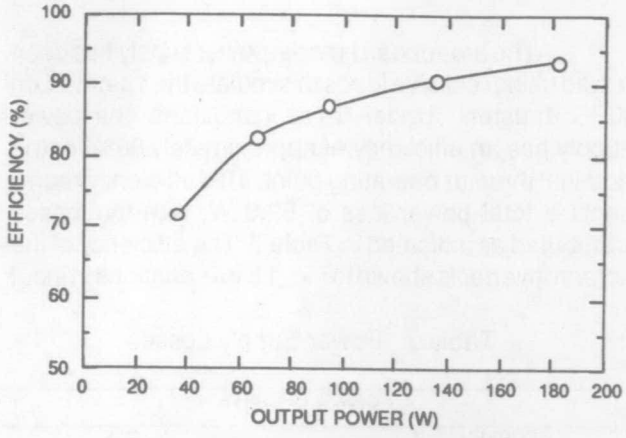

Fig. 12. Efficiency of ac current source.

THRUSTER QUALIFICATION

A photograph of the two qualification-model XIPS thrusters is presented as Fig. 13. These units have been built according to flight-hardware standards and will enter an extended qualification test program later this year. The testing will include performance mapping of both thrusters operated with breadboard-model power supplies, such as the one shown in the photograph of Fig. 14. One of the qualification-model thrusters will be subjected to environmental testing, including thermal vacuum and vibration. Then both units will be subjected to a cyclic lifetest, in which they will operate simultaneously for about 1.9 h ON (in simulation of a typical daily in-orbit firing) and 0.5 h OFF (to permit cool down and accelerated accumulation of test time). Using these ON/OFF segments will result in the accumulation of 10 cycles per day, so that one year of testing will be equivalent to 10 years of operational use. We plan to continue the cyclic testing for approximately 18 months, accumulating 1.5 times the typical required mission life on the two qualification-model thrusters and breadboard-model power supplies.

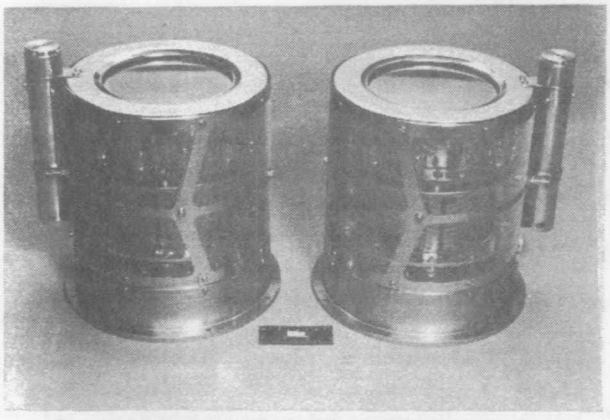

Fig. 13. Qualification-model thrusters.

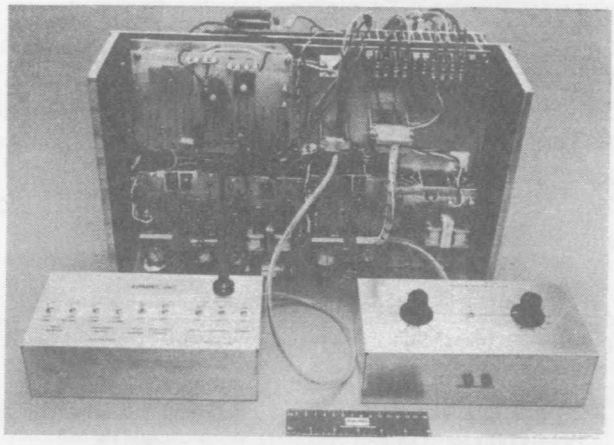

Fig. 14. Breadboard-model power supply.

We also plan to conduct a long-term test of two discharge hollow cathodes. This testing will be performed in an off-line vacuum test chamber, using the discharge-chamber simulators shown in Fig. 15. The simulators replicate the discharge chamber used in the qualification-model thrusters, except that the ion extraction assembly is replaced with a mask having a single on-axis aperture. The area of this aperture is selected so that the nominal cathode emission current and cathode flow rate listed in Table 4 will give a 28- to 30-V discharge voltage and an ion saturation current to the mask approximately equal to the nominal beam current of 405 mA. In this manner, we seek to duplicate conditions within the discharge chamber (i.e., magnetic field, plasma density, gas density, and sputtering rates) that are fully representative of thruster operation under conditions of ion beam extraction.

Fig. 15. Discharge chamber simulators.

SUMMARY

We have described the 18-mN XIPS that we are developing for NSSK on both spin-stabilized and three-axis-stabilized communications satellites. The design approach and development status of the 13-cm-diam thruster and its simplified power supply have been reviewed, and performance data obtained with laboratory and engineering models of the thruster and a breadboard model of the power supply have been shown to confirm the high level of performance anticipated for the XIPS. Our plans to qualify the thruster were presented, along with a description of the qualification-model thrusters and the discharge-chamber simulators that will be used in demonstrating hollow cathode lifetime.

ACKNOWLEDGMENTS

The authors wish to acknowledge G.H Fehlhauer, S. Kami, B.J. Reeves, P.W. Sumner, and A.R. Ward for their efforts in designing, fabricating, and assemblying the XIPS thrusters and discharge chamber simulators. We also acknowledge D.J. Hancock, D.A. Lewis, and M.W. Sawins for fabricating and assemblying the XIPS power supplies.

REFERENCES

1. Beattie, J.R., et al., "Xenon Ion Propulsion Subsystem," *J. Propulsion and Power* 5, pp. 438-444, July-Aug. 1989.

2. Beattie, J.R., Matossian, J.N., and Robson, R.R., "Status of Xenon Ion Propulsion Technology," *J. Propulsion and Power* 6, pp. 145-150, March-April 1990.

3. Beattie, J.R. and Matossian, J.N., "Xenon Ion Propulsion for Stationkeeping and Orbit Raising," DGLR/AIAA/JSASS Paper No. IEPC-88-052, Oct. 3-6, 1988.

4. Sovey, J.S., "Improved Ion Containment Using a Ring-Cusp Ion Thruster," *J. of Spacecr. &Rockets* 21, pp. 488-495, Sept.-Oct.1984.

5. Kaufman, H.R., "Technology of Electron Bombardment Ion Thrusters," in Advances in Electronics and Electron Physics, Vol. 36, Academic Press, edited by L. Marton, 1974.